COBEM 2021 26th International Congress of Mechanical Engineering

ABCM Associação Brasileira de Engenharia e Ciências Mecânicas
November 22-26, 2021, Virtual Congress, Brazil

COB-2021-1011
Evaluation of Control Allocation Methods for Multirotor Aerial Vehicles

José Agnelo Bezerra [1]
Davi A. Santos [2]

Instituto Tecnológico de Aeronáutica
Praça Marechal Eduardo Gomes, 50
São José dos Campos/SP - Brasil
[1] agnelo@ita.br, [2] davists@ita.br

Abstract. *The present work deals with the control allocation of multirotor aerial vehicles (MAVs). We propose an optimal method that directly considers, as a hard equality constraint, the structural relation (control allocation equation) between the rotor commands and the control variable, besides respecting the physical or operational limits of the rotors. The proposed approach aims to exactly allocate the desired control efforts, thus ensuring the designed control features (e.g., performance and stability) for the closed-loop system. The method is compared with three control allocators most used in the aerospace literature: the pseudo-inverse, the direct allocation, and the conventional optimal allocator. Through computational simulations, we can attest that the proposed control allocator performs quite similar to the best existing approaches, but, different from the others, it also guarantees an exact control allocation.*

Keywords: *multirotor aerial vehicle, control allocation*

1. INTRODUCTION

Multirotor aerial vehicles (MAVs) with fixed and parallel rotors have under-actuated dynamics, since they are modeled with six degrees of freedom (DOFs), being three for translation and three others for rotation, but they are actuated by four independent efforts, which are a thrust magnitude and a three-dimensional torque. Inspired by the aerospace literature Durham (1993); Bodson (2002); Oppenheimer *et al.* (2006), the flight control of such vehicles commonly adopts a hierarchical framework composed of control laws, which provide commands for the aforementioned efforts, and a control allocator, which distributes these commands among the rotors Hua *et al.* (2013); Naldi *et al.* (2017). Therefore, for this architecture being effective, an exact control allocation is required, *i.e.*, the resultant commands assigned to the actuators must exactly match the desired efforts given by the control laws.

The control allocation equation of under-actuated MAVs is in general expressed as a linear statement between the four independent control efforts and the individual thrusts of the rotors. Therefore, in the MAV literature, the simplest control allocation approach is found for quadrotors and consists of directly inverting the control allocation equation Mahony *et al.* (2012); Invernizzi *et al.* (2020); Kidambi *et al.* (2021); Ghignoni *et al.* (2021). On the other hand, the same method cannot be applied to vehicles with more than four rotors, since they have actuation redundancy, *i.e.*, their rotor-set has multiple actuation possibilities to generate the same control efforts. In this case, a common approach is to calculate the (weighted) minimum-norm rotor commands that result in the desired control efforts, which is equivalent to enforcing the (weighted) pseudo-inversion of the control allocation equation Ducard and Hua (2011); Santos and Cunha (2019); Ryll *et al.* (2020). Since the rotors have in practice physical limits, the commands of the pseudo-inverse (or inverse) method need to be post-saturated to avoid violating these bounds, which however leads to an inexact control allocation.

A control allocation method that directly considers the physical limits of the rotors is employed in Monteiro *et al.* (2016); Smeur *et al.* (2017); Kirchengast *et al.* (2018). It consists of solving a quadratic optimization that aims to minimize the rotor commands magnitude while assuming those bounds as inequality constraints. To ensure this problem feasibility, an allocation error w.r.t. the desired control efforts is admitted, and this error norm is also minimized in the cost function. Therefore, since the control allocation equation is not considered as a hard constraint, this approach also allows an inexact control allocation, which is an issue that can degrade the closed-loop properties otherwise assured by the control laws (*e.g.*, performance and stability).

The present paper proposes a novel exact optimal control allocator for under-actuated MAVs with fixed and parallel rotors. The proposed approach consists of solving a quadratic optimization where the control allocation equation is explicitly considered as an equality constraint, and the rotor bounds are assumed as inequality constraints. Based on computational simulations, we compare the proposed method with three existing control allocators: the pseudo-inverse, the direct allocation, and the conventional optimal approach. Therefore, we can show that our strategy always provides an exact allocation of the efforts demanded by the control laws, different from all the above-cited papers.

The remaining text is organized in the following manner. Section 2. defines the control allocation problem. Section 3. formulates the proposed optimal control allocator. Section 4. presents the simulation results of the compared control allocators. Finally, Section 5. concludes the paper.

2. PROBLEM STATEMENT

This section is organized as follows: Subsection 2.1 describes the adopted notation; Subsection 2.2 presents the rotor configuration of a generic under-actuated MAV; and Subsection 2.3 enunciates the control allocation problem.

2.1 Notation

The set of (non-negative) real numbers is denoted by $\mathbb{R}$ ($\mathbb{R}_+$). The set of the first n positive integers is denoted by $\mathcal{I}_n \triangleq \{1, 2, ..., n\}$. Scalar quantities are denoted by lowercase italic letters, *e.g.*, $v \in \mathbb{R}$. Vector quantities are represented by lowercase boldface letters, *e.g.*, $\mathbf{v} \in \mathbb{R}^n$, and matrices with arbitrary dimensions are represented by uppercase boldface letters, *e.g.*, $\mathbf{A} \in \mathbb{R}^{n\times m}$. An algebraic vector can be described by $\mathbf{v} = (v_1, v_2, \ldots, v_n)$, where $v_i, \forall i \in \{1, 2, \ldots, n\}$, are its components. The transpose of a matrix $\mathbf{A}$ is denoted by $\mathbf{A}^{\mathrm{T}}$. The $n \times n$ identity matrix is denoted by $\mathbf{I}_n$, while $n \times m$ zero matrices are denoted by $\mathbf{0}_{n\times m}$. Coordinate-free geometric (or physical) vectors are denoted as $\vec{v}$, while versors (with unit magnitude) are denoted as $\hat{v}$. Cartesian coordinate systems (CCSs) are denoted as $\mathcal{S}_b \triangleq \{B; \hat{x}_b, \hat{y}_b, \hat{z}_b\}$, where B represents its origin and the versors $\hat{x}_b$, $\hat{y}_b$, and $\hat{z}_b$ form an orthonormal basis for the three-dimensional space. The algebraic vector resulting from the projection of $\vec{v}$ onto $\mathcal{S}_b$ is represented by $\mathbf{v}_b \in \mathbb{R}^3$, which is referred to as the $\mathcal{S}_b$ representation of $\vec{v}$. The canonical basis for $\mathbb{R}^3$ is represented by the vectors $\mathbf{e}_1 \triangleq (1, 0, 0)$, $\mathbf{e}_2 \triangleq (0, 1, 0)$, and $\mathbf{e}_3 \triangleq (0, 0, 1)$. Finally, consider the $\mathcal{S}_b$ representations $\mathbf{v}_b \triangleq (v_1, v_2, v_3)$, $\mathbf{u}_b$, and $\mathbf{w}_b$ of $\vec{v}$, $\vec{u}$ and $\vec{w} \triangleq \vec{v} \times \vec{u}$, respectively. It holds that $\mathbf{w}_b = [\mathbf{v}_b\times]\mathbf{u}_b$, where $[\mathbf{v}_b\times] \in \mathbb{R}^{3\times 3}$ is the skew-symmetric matrix Shuster (1993)

$$[\mathbf{v}_b\times] \triangleq \begin{bmatrix} 0 & -v_3 & v_2 \\ v_3 & 0 & -v_1 \\ -v_2 & v_1 & 0 \end{bmatrix}.$$

2.2 Rotor-Set Modeling

Consider a generic under-actuated MAV with n_r rotors, as illustrated in Fig. 1. The rotors, in turn, are assumed to be single-mounted, non-reversing, and fixed to the vehicle's structure. Moreover, consider a body-fixed reference frame described by $\mathcal{S}_b \triangleq \{B; \hat{x}_b, \hat{y}_b, \hat{z}_b\}$, which is centered on the vehicle's center of mass B. The versor $\hat{x}_b$ indicates the longitudinal direction, while $\hat{z}_b$ is the body's vertical axis. Assuming that all the rotors are aligned with $\hat{z}_b$, the thrust force and reaction torque produced by the ith rotor are modeled, respectively, by Mahony *et al.* (2012)

$$\vec{f}_i = k_f \omega_i^2 \hat{z}_b, \tag{1}$$
$$\vec{\tau}_i = (-1)^{i+1} k_\tau \omega_i^2 \hat{z}_b, \tag{2}$$

where $k_f \in \mathbb{R}_+$ and $k_\tau \in \mathbb{R}_+$ are aerodynamic coefficients, and $\omega_i \in \mathbb{R}_+$ denotes the spinning rate of the ith rotor. Without loss of generality, for notation simplicity, we assume that all the rotors have the same values of k_f and k_τ.

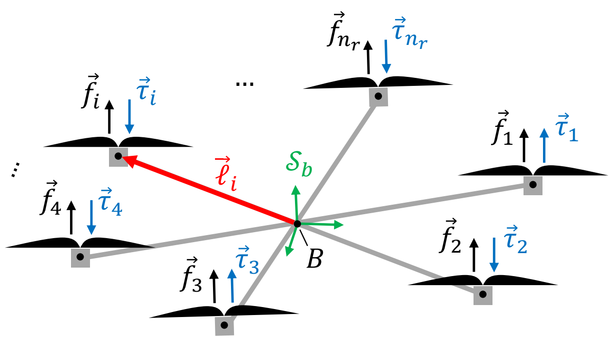

Figure 1. Schematic representation of a generic under-actuated MAV. The black and blue arrows represent the positive directions of the respective quantities.

Given the individual efforts in (1)–(2), the resulting control force and torque acting on the MAV can be expressed, respectively, as

$$\vec{f}^{\,c} = \sum_{i=1}^{n_r} \vec{f}_i, \tag{3}$$

$$\vec{\tau}^{\,c} = \sum_{i=1}^{n_r} \left(\vec{\ell}_i \times \vec{f}_i + \vec{\tau}_i \right), \tag{4}$$

where $\vec{\ell}_i$ is the arm vector of the ith rotor w.r.t B, with $i \in \mathcal{I}_{n_r} \triangleq \{1, 2, \ldots, n_r\}$.

Consider that $\mathbf{f}_b^c \in \mathbb{R}^3$ and $\boldsymbol{\tau}_b^c \in \mathbb{R}^3$ are, respectively, the $\mathcal{S}_b$ representations of $\vec{f}^{\,c}$ and $\vec{\tau}^{\,c}$. Therefore, by replacing (1)–(2) into (3)–(4), we obtain

$$\mathbf{f}_b^c = \sum_{i=1}^{n_r} f_i \mathbf{e}_3, \tag{5}$$

$$\boldsymbol{\tau}_b^c = \sum_{i=1}^{n_r} f_i \left([\boldsymbol{\ell}_{i,b} \times] + k(-1)^{i+1} \mathbf{I}_3 \right) \mathbf{e}_3, \tag{6}$$

where $k \triangleq k_\tau / k_f$, $f_i \triangleq k_f \omega_i^2$ is the magnitude of $\vec{f}_i$, and $\boldsymbol{\ell}_{i,b} \in \mathbb{R}^3$ is the $\mathcal{S}_b$ representation of $\vec{\ell}_i$.

Finally, assume that the spinning rates of the rotors are bounded according to

$$\omega^{\min} \leq \omega_i \leq \omega^{\max}, \tag{7}$$

where $\omega^{\min} \in \mathbb{R}_+$ and $\omega^{\max} \in \mathbb{R}_+$ are assumed to be known.

2.3 Control Allocation Problem

Consider the availability of a flight control law which produces the commands $\bar{f}^c \in \mathbb{R}_+$ and $\bar{\boldsymbol{\tau}}_b^c \in \mathbb{R}^3$ for, respectively, $f^c \triangleq \|\mathbf{f}_b^c\|$ and $\boldsymbol{\tau}_b^c$. The control allocation for under-actuated MAVs consists, in general, in the computation of the spinning rate commands $\bar{\omega}_i$, $i \in \mathcal{I}_{n_r}$, which realize $\bar{f}^c$ and $\bar{\boldsymbol{\tau}}_b^c$. Therefore, by relating these commands in the same way that the respective physical quantities are related in (5)–(6), we can obtain the *control allocation equation*:

$$\mathbf{u} = \boldsymbol{\Gamma} \bar{\mathbf{f}}, \tag{8}$$

where $\mathbf{u} \triangleq \left(\bar{f}^c, \bar{\boldsymbol{\tau}}_b^c \right) \in \mathbb{R}^4$ is the control vector and $\bar{\mathbf{f}} \triangleq \left(\bar{f}_1, \bar{f}_2, ..., \bar{f}_{n_r} \right) \in \mathbb{R}^{n_r}$, with $\bar{f}_i \triangleq k_f \bar{\omega}_i^2$, is the vector of rotor commands. Moreover, the *control allocation matrix* $\boldsymbol{\Gamma} \in \mathbb{R}^{4 \times n_r}$ is given by

$$\boldsymbol{\Gamma} \triangleq \begin{bmatrix} 1 & 1 & \cdots & 1 \\ \boldsymbol{\gamma}_1 & \boldsymbol{\gamma}_2 & \cdots & \boldsymbol{\gamma}_{n_r} \end{bmatrix}, \tag{9}$$

with $\boldsymbol{\gamma}_i \triangleq \left([\boldsymbol{\ell}_{i,b} \times] + k(-1)^{i+1} \mathbf{I}_3 \right) \mathbf{e}_3 \in \mathbb{R}^3$.

For control design purpose, we assume as usual that the rotor dynamics is much faster than the MAV translational and rotational dynamics. Therefore, we can neglect the rotor dynamics in the control allocation, thus resulting in $\omega_i \equiv \bar{\omega}_i$.

Now, we can define the control allocation problem.

Problem 1. Given a control vector $\mathbf{u}$, the control allocation objective is to find some spinning rate commands $\bar{\omega}_i$, $i \in \mathcal{I}_{n_r}$, which satisfies (7)–(8).

3. PROBLEM SOLUTION

This section proposes an optimal control allocator to solve Problem 1. Furthermore, we also formulate some common methods of the literature which have been used to solve the same problem.

Since the control allocation equation (8) is linear in $\bar{\mathbf{f}}$, it is convenient to consider this quantity as the allocation variable, thus resulting in simple and efficient linear control allocators. Therefore, from (7), we can obtain equivalent bounds in terms of $\bar{\mathbf{f}}$

$$\bar{\mathbf{f}}^{\min} \leq \bar{\mathbf{f}} \leq \bar{\mathbf{f}}^{\max}, \tag{10}$$

where $\bar{\mathbf{f}}^{\min} \triangleq \bar{f}^{\min} \mathbf{1}_{n_r}$, $\bar{\mathbf{f}}^{\max} \triangleq \bar{f}^{\max} \mathbf{1}_{n_r}$, $\bar{f}^{\min} \triangleq k_f \left(\bar{\omega}^{\min} \right)^2$, and $\bar{f}^{\max} \triangleq k_f \left(\bar{\omega}^{\max} \right)^2$, with $\mathbf{1}_{n_r} \triangleq (1, \ldots, 1) \in \mathbb{R}_{n_r}$.

With the thrust commands $\bar{f}_i$, $i \in \mathcal{I}_{n_r}$, we can calculate the spinning rate commands, by definition, as follows

$$\bar{\omega}_i = \sqrt{\frac{\bar{f}_i}{k_f}}. \tag{11}$$

The remaining section is organized as follows: Subsection 3.1 presents the pseudo-inverse method; Subsection 3.2 details the direct allocation approach; Subsection 3.3 formulates the conventional optimal method; and Subsection 3.4 proposes a novel optimal control allocator.

3.1 Pseudo-Inverse Method

The most common control allocator in the MAV literature is the pseudo-inverse method (and its variations). It consists in inverting the control allocation equation (8) by means of the pseudo-inverse of matrix $\mathbf{\Gamma}$, as follows

$$\bar{\mathbf{f}}^* = \mathbf{\Gamma}^\dagger \mathbf{u}, \tag{12}$$

with $\bar{\mathbf{f}}^* \triangleq \left(\bar{f}_1^*, \bar{f}_2^*, ..., \bar{f}_{n_r}^*\right)$ and $\mathbf{\Gamma}^\dagger \triangleq \mathbf{\Gamma}^{\mathrm{T}}(\mathbf{\Gamma}\mathbf{\Gamma}^{\mathrm{T}})^{-1} \in \mathbb{R}^{n_r \times 4}$.

Since the bounds of (10) are not considered in the above calculation of $\bar{\mathbf{f}}^*$, this vector can violate those limits, thus yielding unattainable rotor commands. To prevent this issue, the pseudo-inverse method requires a saturation of the rotor commands based on (10), as follows

$$\bar{\mathbf{f}} = \mathrm{sat}_{\mathcal{F}}\left(\bar{\mathbf{f}}^*\right), \tag{13}$$

where $\mathrm{sat}_{\mathcal{F}} : \mathbb{R}_{n_r} \to \mathbb{R}_{n_r}$ is the saturation function in the set $\mathcal{F} \triangleq \left\{\bar{\mathbf{f}} \in \mathbb{R}_{n_r} : \bar{\mathbf{f}}^{\min} \leq \bar{\mathbf{f}} \leq \bar{\mathbf{f}}^{\max}\right\}$.

3.2 Direct Allocation

Direct allocation is a classical method most used in aerospace applications Durham (1993); Bodson (2002). In such cases, it is desirable to preserve the direction of the control command $\mathbf{u}$. Therefore, this method employs a scaling factor $\alpha \in [0, 1]$ and aims to provide the actuator command $\bar{\mathbf{f}}$ related to the maximal value of α, thus resulting in the linear optimization

$$(\bar{\mathbf{f}}^*, \alpha^*) = \underset{(\bar{\mathbf{f}},\alpha)}{\mathrm{argmin}} \quad -\alpha \tag{14}$$

$$\text{subject to} \quad \mathbf{\Gamma}\bar{\mathbf{f}} = \alpha\mathbf{u} \tag{15}$$

$$\bar{\mathbf{f}}^{\min} \leq \bar{\mathbf{f}} \leq \bar{\mathbf{f}}^{\max} \tag{16}$$

$$0 \leq \alpha \leq 1 \tag{17}$$

where $\bar{\mathbf{f}}^* \in \mathbb{R}^{n_r}$ is the optimal vector of rotor commands and $\alpha^* \in [0, 1]$ is the optimal scaling factor.

We can note that, if $\alpha^* = 1$, this method provides an exact control allocation, *i.e.*, $\mathbf{\Gamma}\bar{\mathbf{f}}^* \equiv \mathbf{u}$. However, if $\alpha^* < 1$, this method allows an allocation error of $(1 - \alpha^*)\,\mathbf{u}$.

3.3 Conventional Optimal Control Allocator

Based on the references Monteiro *et al.* (2016); Smeur *et al.* (2017); Kirchengast *et al.* (2018), an optimal control allocator can be formulated as the following quadratic program

$$\bar{\mathbf{f}}^* = \underset{\bar{\mathbf{f}}}{\mathrm{argmin}} \quad \|\bar{\mathbf{f}} - \bar{\mathbf{f}}^{\mathrm{ref}}\|_{\mathbf{Q}}^2 + \|\mathbf{\Gamma}\bar{\mathbf{f}} - \mathbf{u}\|^2 \tag{18}$$

$$\text{subject to} \quad \bar{\mathbf{f}}^{\min} \leq \bar{\mathbf{f}} \leq \bar{\mathbf{f}}^{\max} \tag{19}$$

where $\mathbf{Q} \in \mathbb{R}^{n_r \times n_r}$ is a weighting matrix, $\bar{\mathbf{f}}^{\mathrm{ref}} \in \mathbb{R}^{n_r}$ is a vector of reference thrust commands, and $\bar{\mathbf{f}}^* \in \mathbb{R}^{n_r}$ is the (optimal) rotor command vector. Here, we assume $\bar{\mathbf{f}}^{\mathrm{ref}}$ as the thrust vector for an equilibrium condition (hovering), which is given by $\bar{\mathbf{f}}^{\mathrm{ref}} = mg/n_r\mathbf{1}_{n_r}$, where $m \in \mathbb{R}_+$ is the vehicle's mass and $g \in \mathbb{R}_+$ is the local gravity.

As discussed in Section 1., this optimal control allocator allows an allocation error w.r.t. the control vector $\mathbf{u}$. However, by a proper selection of the weighting matrix $\mathbf{Q}$, this method can provide minor allocation errors.

3.4 Proposed Method

The proposed method is formulated as an optimal control allocator similar to the one in Subsection 3.3. The difference here lies in the consideration of the control allocation equation (8) as a hard equality constraint. With this setting, we aim to ensure an exact allocation of the control vector $\mathbf{u}$, for any admissible condition. As follows, we present the proposed quadratic program

$$\bar{\mathbf{f}}^* = \underset{\bar{\mathbf{f}}}{\text{argmin}} \quad \|\bar{\mathbf{f}}\|^2 \tag{20}$$

$$\text{subject to} \quad \boldsymbol{\Gamma}\bar{\mathbf{f}} = \mathbf{u} \tag{21}$$

$$\bar{\mathbf{f}}^{\min} \leq \bar{\mathbf{f}} \leq \bar{\mathbf{f}}^{\max} \tag{22}$$

where $\bar{\mathbf{f}}^* \in \mathbb{R}^{n_r}$ is the (optimal) rotor command vector.

Based on the previous optimization problem, we can define the *admissible set* as

$$\mathcal{A} \triangleq \left\{ \mathbf{u} \in \mathbb{R}^4 : \exists \bar{\mathbf{f}} \in \mathbb{R}^{n_r} \text{ s.t. } \boldsymbol{\Gamma}\bar{\mathbf{f}} = \mathbf{u}, \bar{\mathbf{f}}^{\min} \leq \bar{\mathbf{f}} \leq \bar{\mathbf{f}}^{\max} \right\}. \tag{23}$$

It is possible to show that the proposed control allocator is feasible if and only if $\mathbf{u} \in \mathcal{A}$. In other words, the adopted control law must provide an admissible control vector $\mathbf{u}$, so that the control allocator can calculate rotor commands satisfying (8) and (10). Furthermore, we note that many controllers can explicitly take the control bounds into account, *e.g.*, the model predictive control Rawlings *et al.* (2017), an outer control layer that ensures the satisfaction of constraints Bezerra and Santos (2021), or a stabilizing control law under saturation Santos *et al.* (2013); Santos and Cunha (2019).

4. SIMULATION RESULTS

In order to test the proposed control allocator, we consider an under-actuated hexa-rotor aerial vehicle, whose rotors are fixed and parallel to $\hat{z}_b$. The physical parameters of the vehicle are: $\ell = 0.4\,\text{m}$, $k_f = 2.5 \times 10^{-5}\,\text{kg}\,\text{m}$, $k_\tau = 5.0 \times 10^{-7}\,\text{kg}\,\text{m}^2$, mass of $1\,\text{kg}$, and inertia matrix of $\text{diag}([0.015, 0.015, 0.030])\text{kg}\,\text{m}^2$. Moreover, the rotor bounds of (7) are considered as $\omega^{\min} = 40\,\text{rad/s}$ and $\omega^{\max} = 400\,\text{rad/s}$.

The results of this section were obtained through simulations in MATLAB, using the Euler integrator to solve the vehicle dynamics, with time step $0.01\,\text{s}$. By means of the MATLAB function *quadprog*, the algorithm *interior-point-convex*, with constraint tolerance of 1×10^{-8}, was used to solve the quadratic problems of (18)–(19) and (20)–(22). On the other hand, the linear optimization of (14)–(17) was solved using the function *linprog*, by means of the algorithm *dual-simplex* with constraint tolerance of 1×10^{-12}.

Initially, the four methods described in Section 3. are compared through a static simulation, which consists in solving the related control allocation problems for 1000 random samples of $\mathbf{u}$ drawn from $\mathcal{A}$. The results of this simulation are summarized in Tab. 1.

Table 1. Results of the static simulation. The values are given in SI units.

Method	Violations	Mean/Max Force Error	Mean/Max Torque Error	Mean/Max Time
proposed method	0	$1.2 \times 10^{-11}/1.7 \times 10^{-9}$	$3.7 \times 10^{-12}/4.5 \times 10^{-10}$	$2.1 \times 10^{-3}/5.4 \times 10^{-3}$
pseudo-inverse	519	$1.7 \times 10^{-1}/1.1$	$6.3 \times 10^{-2}/4.3 \times 10^{-1}$	$1.8 \times 10^{-5}/3.0 \times 10^{-4}$
optimal allocation	0	$1.1 \times 10^{-2}/2.0 \times 10^{-2}$	$2.3 \times 10^{-7}/4.1 \times 10^{-5}$	$1.3 \times 10^{-3}/3.0 \times 10^{-3}$
direct allocation	0	$1.2 \times 10^{-15}/7.1 \times 10^{-15}$	$1.2 \times 10^{-15}/3.6 \times 10^{-15}$	$7.3 \times 10^{-3}/1.5 \times 10^{-2}$

In the second column of Tab. 1, the number of violations of the rotor bounds (7), for each control allocator, is reported. Since the pseudo-inverse allocator is the only method that does not directly take inequality constraints into account, it violated those bounds in 51.9% of the trials, while no violation was observed for the other methods. This fact enforces the need to saturate the pseudo-inverse commands according to the actuator limits.

The allocation errors of force and torque are presented, respectively, in the third and fourth columns. The pseudo-inverse method verified the greatest errors, which are caused by the required saturation of commands. The conventional optimal allocator also verified significant allocation errors, which are induced by the formulation with the control allocation equation in the cost, instead of considering it as a hard constraint. On the other hand, the direct allocation and the proposed method observed errors below the respective solver tolerance, thus they are related to numerical approximations.

The computational time demanded by the allocation methods is reported in the last column of Tab. 1. Since the pseudo-inverse approach has a closed-form solution, it requires fewer computations than the others, resulting in the least execution time. The three other methods showed to be two orders of magnitude slower, although the observed times are still viable for real-time implementation.

Now, the control allocation methods are also compared through a dynamic simulation. In this case, the previously described hexa-rotor starts with null states and is abruptly commanded to the condition with heading angle of $45\,^\circ$ and position of $(1, 1, 1)\,\text{m}$. The position and attitude controllers are the same for all control allocators, consisting of inverse-dynamic laws with PD actions and post-saturation in the admissible set $\mathcal{A}$. The results of this simulation are illustrated in Figs. 2–4.

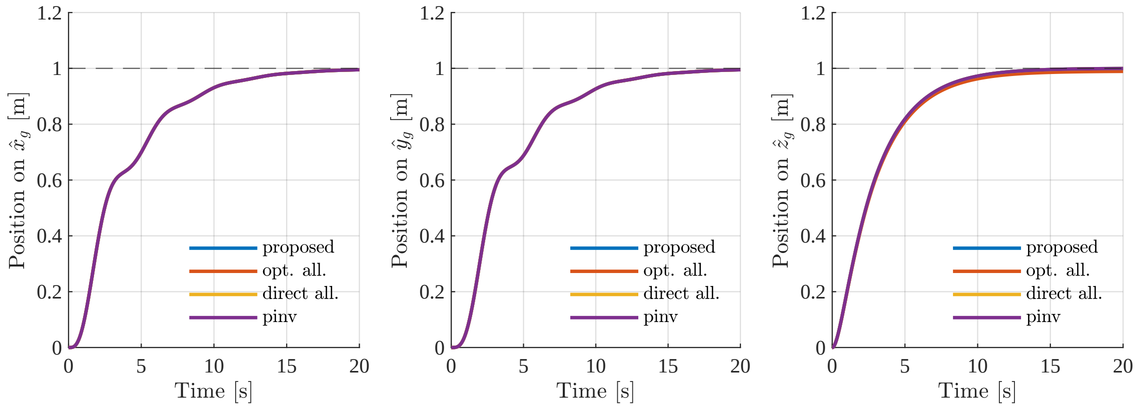

Figure 2. Position of the hexa-rotor during simulation. The waypoint's position is represented as a dashed black line.

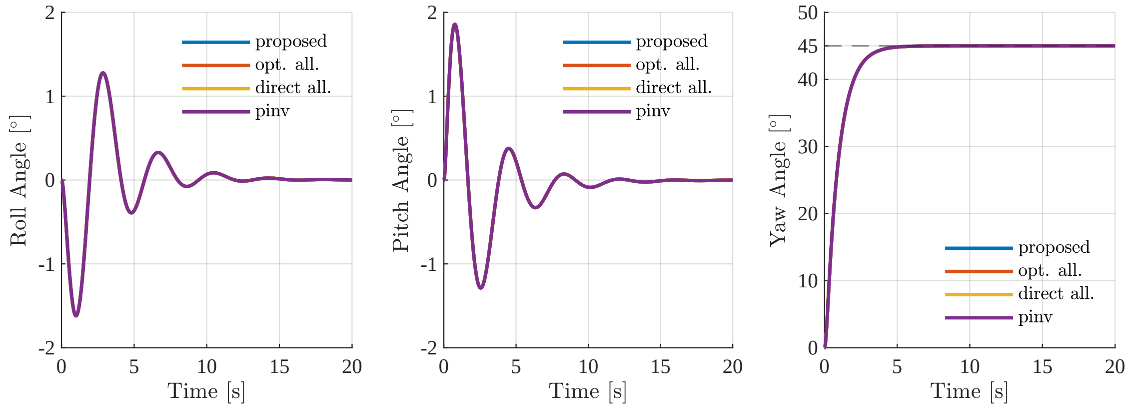

Figure 3. Attitude (in Euler angles 123) of the hexa-rotor during simulation. The waypoint's angle is represented as a dashed black line.

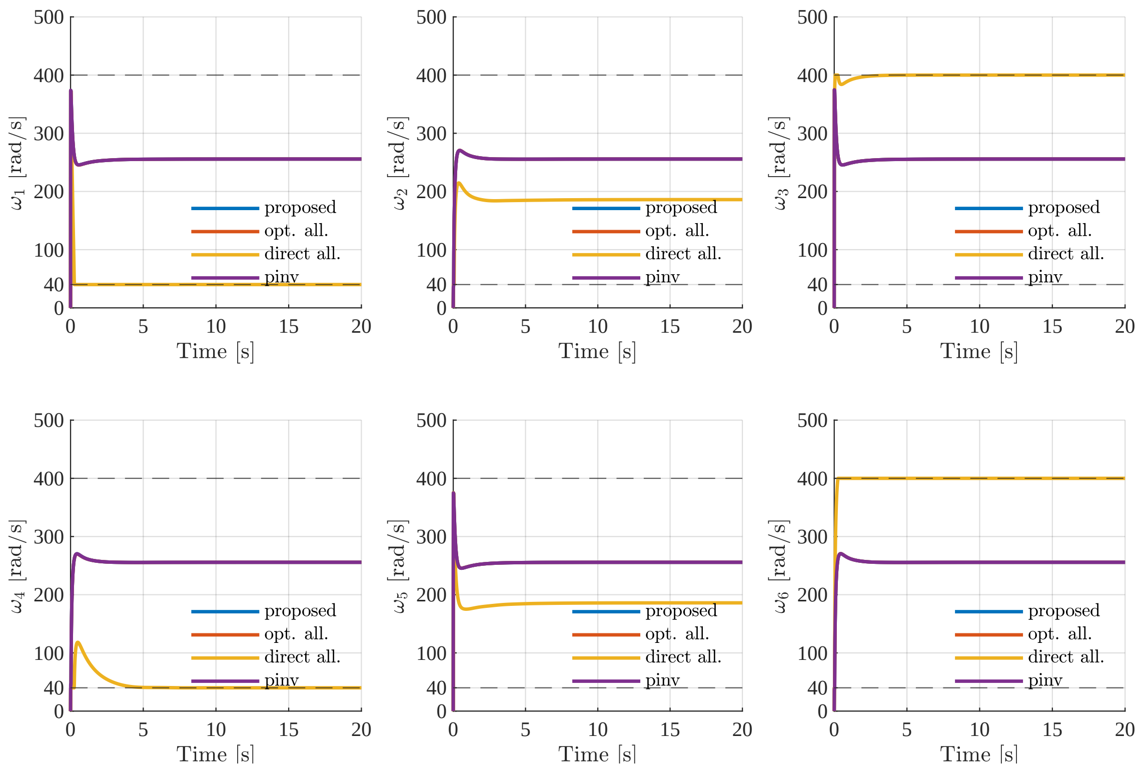

Figure 4. Spinning rate of the rotors during simulation. The rotor bounds are represented as dashed black lines.

Using Figs. 2–3, we can note that the MAV states have a quite close behavior in all the cases. The most significant difference lies for the conventional optimal allocator, which presented a nonzero steady-state error for the position in $\hat{z}_g$ direction. On the other hand, Fig. 4 shows that the control allocators commanded the rotors in different ways. For all the methods, except the direct allocation, the six rotors assumed the same steady-state spinning rate of $(mg/n_r k_f)^{1/2} = 255.7\,\mathrm{rad/s}$. The direct allocation, in turn, commanded two of the rotors to assume the maximum spinning rate in steady-state. Although this control allocation is feasible, it is not desirable in practice, since it can lead the rotors to work in their bounds for a long time, which favors the occurrence of failures. Therefore, the three other approaches showed a better behavior for practical applications.

5. CONCLUSION

In this paper, we have proposed a novel optimal control allocator for under-actuated MAVs. The proposed method is formulated to work with flight control laws that are able of considering control bounds. Using computational simulations, this method has been compared with three existing control allocators. The results have shown that our approach always provides an exact control allocation, besides having a computational burden suitable for real-time implementation. Therefore, we can state that the proposed control allocator is suited for MAV applications with high demands of safety and actuator saving, *e.g.*, aerial manipulation, and delivery. Finally, a further investigation of the method's properties is needed in future work.

6. ACKNOWLEDGEMENTS

The authors would like to thank the São Paulo Research Foundation (FAPESP), for the financial support under grant 2019/05334-0. The first author also thanks to the Brazilian Air Force for the educational and professional support. The second author is also grateful for the support of the Brazilian National Council for Scientific and Technological Development (CNPq), under grant 302637/2018-4.

7. REFERENCES

Bezerra, J.A. and Santos, D.A., 2021. "On the guidance of fully-actuated multirotor aerial vehicles under control allocation constraints using the receding-horizon strategy". *ISA Transactions*. ISSN 0019-0578. doi: https://doi.org/10.1016/j.isatra.2021.07.019.

Bodson, M., 2002. "Evaluation of optimization methods for control allocation". *Journal of Guidance, Control, and Dynamics*, Vol. 25, No. 4, pp. 703–711. doi:10.2514/2.4937.

Ducard, G.J.J. and Hua, M.D., 2011. "Discussion and practical aspects on control allocation for a multi-rotor helicopter". *ISPRS - International Archives of the Photogrammetry, Remote Sensing and Spatial Information Sciences*, Vol. XXXVIII-1/C22, pp. 95–100. doi:10.5194/isprsarchives-XXXVIII-1-C22-95-2011.

Durham, W.C., 1993. "Constrained control allocation". *Journal of Guidance, Control, and Dynamics*, Vol. 16, No. 4, pp. 717–725. ISSN 0731-5090. doi:10.2514/3.21072.

Ghignoni, P., Buratti, N., Invernizzi, D. and Lovera, M., 2021. "Anti-windup design for directionality compensation with application to quadrotor uavs". *IEEE Control Systems Letters*, Vol. 5, No. 1, pp. 331–336. doi: 10.1109/LCSYS.2020.3001881.

Hua, M., Hamel, T., Morin, P. and Samson, C., 2013. "Introduction to feedback control of underactuated vtolvehicles: A review of basic control design ideas and principles". *IEEE Control Systems Magazine*, Vol. 33, No. 1, pp. 61–75. doi:10.1109/MCS.2012.2225931.

Invernizzi, D., Lovera, M. and Zaccarian, L., 2020. "Integral iss-based cascade stabilization for vectored-thrust uavs". *IEEE Control Systems Letters*, Vol. 4, No. 1, pp. 43–48. doi:10.1109/LCSYS.2019.2921535.

Kidambi, K.B., Fermüller, C., Aloimonos, Y. and Xu, H., 2021. "Robust nonlinear control-based trajectory tracking for quadrotors under uncertainty". *IEEE Control Systems Letters*, Vol. 5, No. 6, pp. 2042–2047. doi: 10.1109/LCSYS.2020.3044833.

Kirchengast, M., Steinberger, M. and Horn, M., 2018. "Control allocation under actuator saturation: An experimental evaluation". *IFAC-PapersOnLine*, Vol. 51, No. 25, pp. 48–54. ISSN 2405-8963. doi: https://doi.org/10.1016/j.ifacol.2018.11.080. 9th IFAC Symposium on Robust Control Design ROCOND 2018.

Mahony, R., Kumar, V. and Corke, P., 2012. "Multirotor aerial vehicles: Modeling, estimation, and control of quadrotor". *IEEE Robotics Automation Magazine*, Vol. 19, No. 3, pp. 20–32. doi:10.1109/MRA.2012.2206474.

Monteiro, J.C., Lizarralde, F. and Liu Hsu, 2016. "Optimal control allocation of quadrotor uavs subject to actuator constraints". In *2016 American Control Conference (ACC)*. pp. 500–505. doi:10.1109/ACC.2016.7524963.

Naldi, R., Furci, M., Sanfelice, R.G. and Marconi, L., 2017. "Robust global trajectory tracking for underactuated vtol aerial vehicles using inner-outer loop control paradigms". *IEEE Transactions on Automatic Control*, Vol. 62, No. 1, pp. 97–112. doi:10.1109/TAC.2016.2557967.

Oppenheimer, M.W., Doman, D.B. and Bolender, M.A., 2006. "Control allocation for over-actuated systems". In *2006 14th Mediterranean Conference on Control and Automation*. pp. 1–6. doi:10.1109/MED.2006.328750.

Rawlings, J.B., Mayne, D.Q. and Diehl, M.M., 2017. *Model Predictive Control*. Nob Hill Publishing.

Ryll, M., Bicego, D., Giurato, M., Lovera, M. and Franchi, A., 2020. "Fast-hex – a morphing hexarotor: Design, mechanical implementation, control and experimental validation". Preprint.

Santos, D.A., Saotome, O. and Cela, A., 2013. "Trajectory control of multirotor helicopters with thrust vector constraints". In *21st Mediterranean Conference on Control and Automation*. pp. 375–379. doi:10.1109/MED.2013.6608749.

Santos, D.A. and Cunha, A., 2019. "Flight control of a hexa-rotor airship: Uncertainty quantification for a range of temperature and pressure conditions". *ISA Transactions*, Vol. 93, pp. 268–279. ISSN 0019-0578. doi: https://doi.org/10.1016/j.isatra.2019.03.010.

Shuster, M.D., 1993. "A Survey on Attitude Representations". *Journal of the Astronautical Sciences*, Vol. 41, No. 4, pp. 439–517.

Smeur, E., Hoppener, D. and Wagter, C.D., 2017. "Prioritized Control Allocation for Quadrotors Subject to Saturation". In *International Micro Air Vehicle Conference and Flight Competition (IMAV) 2017*. Toulouse, France, pp. 37–43.

8. RESPONSIBILITY NOTICE

The authors are solely responsible for the printed material included in this paper.